Core Loss Analysis for the Planar Switched Reluctance Motor

J. F. Pan[1], F. J. Meng[1,2], and Norbert Cheung[2]
[1] College of Mechatronics and Control Engineering, Shenzhen University, P.R.C.
[2]Department of Electrical Engineering, Hong Kong Polytechnic University, P.R.C.
3688, Nanhai Road, 518060, P.R.C.
pan_jian_fei@163.com

***Abstract*—Core loss is one of the key factors for evaluation for the performance of switched reluctance machines. In this paper, core loss based on three dimensional (3D) time-stepping finite element methods (FEM) is calculated for the planar switched reluctance motor (PSRM). Corresponding experiments of loss measurement for the PSRM prototype are conducted and the results prove the accuracy from the numerical analysis.**

***Index Terms*—FEM, loss measurement, numerical analysis.**

I. Introduction

Planar motors are suitable for two dimensional (2D), direct-drive applications [1]. Analysis and optimization on planar motors are discussed in [1]-[3]. In [1], characteristic analysis of a long-stroke synchronous permanent magnet planar motor is discussed by using the finite element method (FEM). A novel overlapping ironless windings for analysis and design of permanent magnet planar motors is proposed in [2]. However, few papers have analyzed the losses in planar switched reluctance motors. This paper focuses on the calculation of core loss based on FEM and derivation of average loss by experimental parameters such as voltage, current and force, etc. from the PSRM prototype. The simulation results correlate those from the experiments.

II. Machine Structure and Calculation Method

A. Machine Structure

Fig.1 (a) shows the primary structure of the PSRM prototype, which is mainly composed of silicon steel plates for the planar stator components and the movers. The moving platform consists of two sets of three-phase mover with windings, which are fixed on a holding aluminum plate at the same level.

One method for core loss reduction is to use laminated stator structure [4]. The stator components contain multiple short laminated silicon-steel blocks which are held together by epoxy glue. The matrix is assembled by inserting one leg of the stator component to the leg hole of another one as shown in Fig.1 (b). The flux circulation in 2D can be found in Fig.1 (b) [5].

B. Theoretical Analysis

Core loss P_v in PSRM consists of eddy current loss P_c, hysteresis loss P_h and excess loss P_e [6-7]. In this paper 3-D Time-Stepping Finite Element Analysis (FEA) is applied to calculate the distribution of the copper loss in the coil windings and the core loss in each silicon-steel plate using Ansoft Maxwell 3D. Equation (1-3) are used for core loss computation with $\beta = 2$. Therefore, core loss is greatly influenced by flux density, frequency, and lamination thickness.

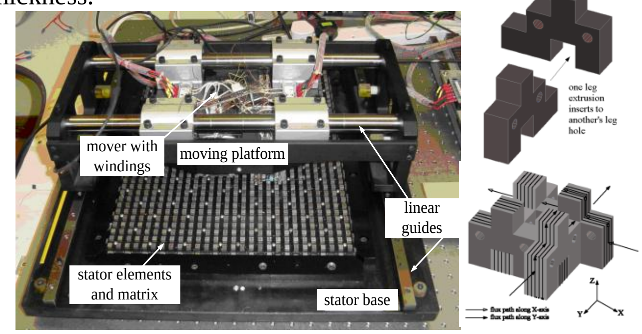

(a) (b)

Fig. 1. Motor prototype (a) and (b) formation of stator matrix and flux circulation

$$P_h(t) = \left\{ \left| H_x \frac{dB_x}{dt} \right|^{2/\beta} + \left| H_y \frac{dB_y}{dt} \right|^{2/\beta} + \left| H_z \frac{dB_z}{dt} \right|^{2/\beta} \right\}^{\beta/2} . \quad (1)$$

$$P_c(t) = \frac{1}{2\pi^2} K_c \left\{ \left(\frac{dB_x}{dt} \right)^2 + \left(\frac{dB_y}{dt} \right)^2 + \left(\frac{dB_z}{dt} \right)^2 \right\} . \quad (2)$$

$$P_e(t) = \frac{1}{C_e} K_e \left\{ \left(\frac{dB_x}{dt} \right)^2 + \left(\frac{dB_y}{dt} \right)^2 + \left(\frac{dB_z}{dt} \right)^2 \right\}^{0.75} . \quad (3)$$

where B, H, K_c and K_e are the amplitude of flux density of the PSRM, the amplitude of the magnetic field strength, the eddy current core loss coefficient and the excess loss coefficient, respectively. The core loss coefficients such as K_c and K_e are defined by electrical properties of steel material and $C_e = 8.763$.

C. 3-D Time-Stepping FEA

For magnetic field analysis and the core loss computation of the PSRM, the magnetization characteristics (B-H curve in Fig.2 (a)) of the electrical steel material is needed and the core loss data sheet of B-P curve as shown in Fig.2 (b) are used to calculate the core loss.

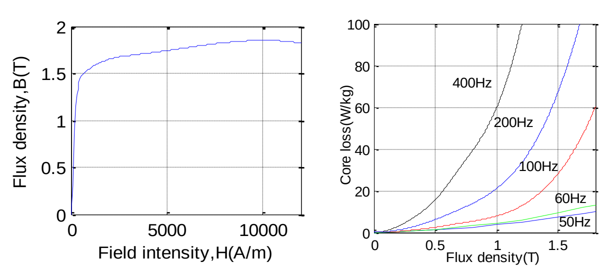

(a) (b)

Fig. 2. Material characteristics (a) B-H curve and (b) B-P curve

III. Results and Discussions

A. Simulation Results from FEM

Since each phase from two axes have the same dimensions and ratings, any one phase can be constructed for FEM simulation. Fig. 3 shows the magnetic flux distribution contour at the unaligned position for the mover relative to the stator with current excitation at 5 A. It can be seen that the flux distributes within the short magnetic path among the mover, the stator area and the air gap region between them. Most of the flux lines penetrate through both the poles and air gaps. To ensure 2D flux circulation perpendicularly, the *LEGO* topology of the stator matrix makes flux flow through the contact regions between stator component legs with glues [5]. Moreover, flux lines distribute mostly in the mover and stator teeth compared to mover and stator yokes. Therefore, there is a higher tendency of saturation from the teeth.

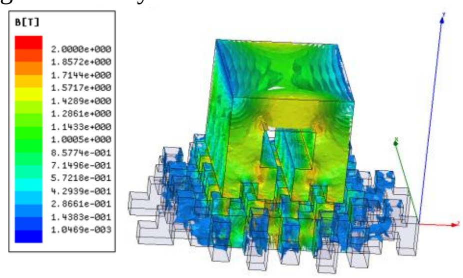

Fig. 3. 3D FEM results of distributions of magnetic flux

B. Experimental Results

For simple and accurate measurement, the speed and mechanical output power are kept constant. The input power is measured as the average of the product of input current to the switching converter and the DC link voltage, while the output power is obtained by multiplying the speed and the constant load of the motor. The copper loss is calculated by multiplying the resistance of the phase winding and the square of current flowing through the phase.

Core loss can be obtained by subtracting the known losses from the measured losses [4]. Core loss from experimental measurement can be represented as,

$$P_{vm} = P_{in} - P_{out} - P_{cu} - P_{fw} - P_{st} \quad (3)$$

where P_{vm} is the measured core loss, P_v is the simulated core loss, P_{in} is the input power, P_{out} is the output power, P_{cu} is the copper loss and P_{fw} is the friction and windage loss. P_{st} is the stray load loss, predicted by the fixed-value method [8] as 0.0906 W and 0.5% of the input power.

Friction and windage losses are independent of the load of the machine. However, they are dependent on the speed of the motor as well as on the air gap and the stack length of the motor. In addition, the normal force makes a significant contribution to the friction and windage loss [6]. Since it is difficult to mount any sensor among the air gaps for accurate measurement of the normal force, FEM is used to calculate the effect of different current excitation levels on normal force P_n at different positions. Coefficient of the kinetic friction of the longitudinal direction μ_x =0.0339 is obtained by measuring the friction and windage force F_{fw} of the PSRM which is driven by a linear actuator at speed constant. Coefficient of kinetic friction of the perpendicular direction μ_y =0.0532 is evaluated as well. The friction and windage losses are measured as the average of the product of normal force times coefficient of kinetic friction multiplied by the constant speed. The measured core loss values can be found in column 4 from Table I at operation speed of 0.05, 0.08 and 0.1 m/s, respectively. It can be concluded that the core loss percentage to the total input power of 27.70%, 30.12% and 32.93% can be derived at different speed, respectively.

TABLE I
CORE LOSS RESULTS OF X AXIS

Speed (m/s)	Measured copper loss (W)	Friction and wingding loss (W)	Measured core loss (W)	Simulated core loss (W)	Pvm/Pin (%)
0.05	10.150	0.622	4.155	3.288	27.70
0.08	11.539	1.033	5.458	5.928	30.12
0.1	15.870	1.126	8.554	8.273	32.93

IV. Conclusions

In this paper, core loss of the PSRM prototype has been investigated using 3D time-stepping FEM and results are verified by the experiment. Experimental results agree with the analytical simulation data. Since core loss is a significant part of the total magnetic losses in a PSRM, it is essential for the design of efficient PSRMs with accurate results.

V. Acknowledgement

The authors would like to thank the National Natural Science Foundation of China, Guangdong Natural Science Foundation and Hong Kong PolyU Central Research Grant for sponsoring of research projects under the code 51007059, 51275312, S2011010001208 and G-YX2Q.

References

[1] Lu Zhang, Baoquan Kou, He Zhang, Shoulun Guo, "Characteristic analysis of a long-stroke synchronous permanent magnet planar motor," *IEEE Trans. Magn.*, vol. 48, no. 11, pp. 4658-4661, 2012.

[2] Wei Min, Ming Zhang, Yu Zhu, Feng Liu, Guanghong Duan, Jinchun Hu, and Wensheng Yin, "Analysis and design of novel overlapping ironless windings for planar motors," *IEEE Trans. Magn.*, vol. 47, no. 11, pp. 4635-4642, 2011.

[3] Jiayong Cao, Yu Zhu, Wensheng Yin, and Wei Xu, "Electromagnetic forces acting on the planar armature of a core-type synchronous permanent-magnet planar motor," *IEEE Trans. Magn.*, vol. 45, no. 8, pp. 3145–3150, 2009.

[4] D. Lin, P. Zhou, Q. M. Chen, N. Lambert, and Z. J. Cendes, "The effects of steel lamination core losses on 3D transient magnetic fields," *IEEE Trans. Magn.*, vol. 46, No. 8, pp. 3539-3542, 2010.

[5] J.F. Pan, N.C. Cheung, W.C. Gan and S.W. Zhao, "A novel planar switched reluctance motor for industrial applications," *IEEE Trans. Magn.*, vol.42, no. 10, pp. 2836-2839, 2006.

[6] J.T. Charton, J. Corda, J.M. Stephenson, and S.P. Randall, "Dynamic modeling of switched reluctance machines with iron losses and phase interactions," *IET Electric Power Applications*, vol. 153, no. 3, pp. 327-336, 2006.

[7] Emad Dlala, "Comparison of models for estimating magnetic core losses in electrical machines using the finite-element method," *IEEE Trans. Magn.*, vol.45, no. 2, pp. 716-725, 2009.

[8] Gang Tong, and Min Zhai, "Study on Stray Load Losses Algorithm Based on Eh-Star Method," *International Conf. World Automation Congress*, pp. 1-4, 2012.